A Rigorous Protocol with Quantitative Isotope Sensitive Measurements for the Electrochemical Reduction of N_2 to NH_3

Suzanne Z. Andersen[†1], Viktor Čolić[†1], Sungeun Yang[†1], Jay A. Schwalbe[2], Adam C. Nielander[2], Joshua M. McEnaney[2], Kasper Enemark-Rasmussen[3], Jon G. Baker[2], Aayush R. Singh[2], Brian A. Rohr[2], Michael J. Statt[2], Sarah J. Blair[2], Stefano Mezzavilla[1], Jakob Kibsgaard[1], Peter C. K. Vesborg[1], Matteo Cargnello[2], Stacey F. Bent[2], Thomas F. Jaramillo[2], Ifan E. L. Stephens[4], Jens K. Nørskov[2], Ib Chorkendorff*[1].

[1] Department of Physics, Technical University of Denmark, Building 311, Fysikvej, DK-2800 Kgs. Lyngby, Denmark
[2] SUNCAT Center for Interface Science and Catalysis, Department of Chemical Engineering, Stanford University, Stanford, California 94305, United States
[3] Department of Chemistry, Technical University of Denmark, Building 207, DK-2800 Kgs. Lyngby, Denmark
[4] Department of Materials, Imperial College London, London SW7 2AZ, United Kingdom
[†] These authors have contributed equally
*Corresponding author email: Ibchork@fysik.dtu.dk

Electrochemical ammonia synthesis ($N_2 + 6H^+ + 6e^- \rightarrow 2NH_3$) under mild conditions (below 100 ºC and at atmospheric pressure) provides an attractive alternative to the fossil fuel-intensive Haber-Bosch process[1–3], enabling the coupling of *renewable electricity* to ammonia production[4]. However, most experimental studies, thus far, only report small quantities of ammonia, produced with low selectivity, reflecting significant scientific and technical challenges[5,6]. Low quantities of NH_3 observed can easily be confused with ammonia ubiquitous in the environment, which makes it difficult to determine whether or not fixation of molecular nitrogen actually occurred[7–9]. This is especially concerning as ammonia can easily be found in air, human breath, and ion-conducting membranes[9]. Moreover, labile nitrogen-containing compounds, such as nitrates, amines, nitrites, nitrogen oxides, etc., are typically present in the gas stream[10], atmosphere, or even the catalyst itself. The field is in need of a standardized set of control experiments, benchmarking protocols for the reaction, as well as methods to eliminate or quantify contamination sources. Very

recently, and during the submission of this manuscript, others have proposed protocols to address these issues.[11,12] However, those studies do not probe contamination levels from different sources or propose strategies to mitigate the contamination. More importantly, they lack examples of successful electrochemical ammonia synthesis. We propose a rigorous procedure for the reliable detection and quantification of N_2 electroreduction to NH_3, using $^{15}N_2$ as an indispensable step. We show how to perform quantitative isotope measurements, demonstrate experimentally the significance of various sources of contamination, provide a method to remove labile nitrogen-containing compounds present in the N_2 gas, and cycle $^{15}N_2$ gas to reduce both contamination and the cost of isotope measurements. By following this protocol, we both prove a negative result on the most promising pure metal catalysts in aqueous media, and successfully demonstrate and quantify ammonia synthesis using lithium electrodeposition in tetrahydrofuran[13].

To assess the importance of background ammonia, we conducted electrochemical benchmarking experiments on the most promising pure metal catalysts[14], Ru, Re and Rh, in aqueous electrolytes. Those electrochemical experiments, shown in Figure 1, did not yield more ammonia than the background level of ~10 ppb; we thus conclude that under these conditions no ammonia is synthesized. This is due to the competing hydrogen evolution reaction (HER), which dominates in an aqueous environment[5]. Figures 2A-C compares the ammonia levels seen in this negative result with the literature, showing that reported ammonia rates and concentrations are close to common background levels, which we explicitly quantify (see Extended Data Figure 1). We also stress that reporting rates alone in the absence of control experiments is insufficient to ensure reliable results. Scientists in adjacent fields are aware of this problem of spurious nitrogen[15]. Apparent reports of photochemical NH_3 synthesis using TiO_2 could not be reproduced under rigorous measurements[16]. Furthermore, researchers have retested Sn(II) phthalocyanine catalysts for N_2 reduction by including electrode washing procedures and extensive background tests; they suggested that the ammonia arose from contaminants or catalyst decomposition[17]. Consequently, the development of a protocol that distinguishes false positives from breakthroughs is essential[11,12].

We stress that no single control experiment is enough to prove that ammonia has been produced from dinitrogen, rather than adventitious contamination; the dataset as a whole must be considered to assess the accuracy of reported rates. To this end, we implement a systematic benchmarking protocol to quantify N_2 electroduction, presented in Figure 3.

As discussed by others[11,12], control experiments with Ar must be performed under the exact same conditions as the N_2 electroreduction experiments, to quantify ammonia originating from contamination within the cell or the catalyst itself. A control experiment with N_2 at open circuit potential (OCP) for the same duration is also neccessary. However, even high purity N_2 gas can contain ammonia and other more easily reduced nitrogen sources, e.g. NO_x. This source of adventitious contamination can be dealt with by first passing the gas over an appropriate adsorbent, e.g. Cu (see Methods section).

Should activity tests yield a comparable level of ammonia to control tests, then contamination may be present. See Methods section for a detailed description of contamination experiments performed within this study.

For instance (i) Nafion - which some N_2 electroreduction experiments employ as a separating membrane or electrolyte[9,18] - accumulates and releases NH_4^+ through ion exchange with acid groups (see Methods section). (ii) air contains a non negligible amount of ammonia, ranging from 0.05-250 ppm[19]. If chemicals and/or the experimental setup are left open, they can accumulate atmospheric ammonia, so a closed system is therefore imperative to exclude this contamination. (iii) human breath contains 0.3-3.0 ppm ammonia[20]. All these sources of contamination vary enonrmously. To account for ammonia contamination, it is thus necessary to accumulate ammonia in concentrations significantly exceeding the concentration from the control measurements with Ar as well as N_2 at OCP over the same duration. However, to provide more definite proof that the ammonia originates from N_2 electroreduction, it is imperative to conduct isotope labelling measurements using $^{15}N_2$ gas. Not only is it essential to measure $^{15}NH_3$ with an ***isotope sensitive method,*** *but it should also be* in ***quantitative agreement*** with $^{14}N_2$ reduction

tests. Although some of the recent publications in Figure 2 demonstrate isotope labelling experiments, most lack quantitative data; they hence fail the requirements of the protocol described herein.

There are several methods for discriminating $^{15}NH_3$ from $^{14}NH_3$, including mass spectroscopy[21] and IR measurements[22] (see Methods section and Extended Data Figure 3); here we focus on NMR which we found most convenient. ^{1}H NMR can differentiate the isotopes, as the scalar interaction between ^{1}H and ^{15}N in $^{15}NH_4^+$ results in a splitting of the ^{1}H resonance into two symmetric signals with a spacing of 73 Hz, while the ^{1}H resonance coupled to ^{14}N in $^{14}NH_4^+$ is split into three symmetric signals with a spacing of 52 Hz. A solution with no added ammonia still shows faint peaks for $^{14}NH_4^+$, due to the aforementioned background contamination. The peaks for $^{15}NH_4^+$ are distinguishable at concentrations down to 51 ppb under the conditions described in the Methods section using an 800 MHz NMR instrument. The amounts of $^{14}NH_4^+$ and $^{15}NH_4^+$ can be quantified from the integrated areas. We have also demonstrated this strategy using a lower field and more common 400 MHz NMR system (see Extended Data Figure 2).

Isotope labelled $^{15}N_2$ gas is rarely pure, not only containing ammonia as an imputity, but also other more labile nitrogen containing compounds such as NO_x[10]. For example, a recent study reported µg yields of NH_3 during the course of over several days[23]. The isotope labelling test within that study employed $^{15}N_2$ gas with a purity of 99.13%, which was bubbled for 28 hours at 10 ml/min.[23] 0.87% of impurities could conceivably lead to 3,600 µg of ammonia or other nitrogen-containing species per hour, equivalent to 100 mg over the course of the experiment. The said study, like most reports in the literature, neglected such concerns related to impuriries in $^{15}NH_3$. Nonetheless, this example serves to illustrate that such contamination is highly problematic, even if the impurity level is restrictied to a few ppm. As such, this concern necessitates the use of additional purification methods before the gas enters the electrochemical cell. We show that a reduced copper catalyst (see Methods section) can effectively adsorb such impurities. Control measurements with $^{15}N_2$ gas flowing through the cell under OCP must be conducted to establish the level of ammonia contamination from the gas feed, in the same manner as measurements with $^{14}N_2$ gas.

As we have shown in the Methods section, recycling the N_2 offers the benefits of lowering both the impurity level and cost of the $^{15}N_2$.

The results must be reproducible through repeated experiments, enabling the inclusion of error bars, and allowing for determination of mean and variance of the data. To ensure meaningful comparison of data collected under different conditions in different experimental setups, it is necessary to report the actual concentration of detected ammonia, as well as the concentration in control measurements along with the electrolyte volume.

Figures-of-merit, which should be reported include: the partial current density in mA/cm^2, normalised to geometric and/or microscopic surface area; turnover frequency (TOF) per site per second; working electrode potential; Faradaic efficiency; yield rate, particularly per surface area or gram of catalyst.

The amount of ammonia quantified via the isotope specific method must be similar to the amount quantified via the colorimetric method. Most importantly, there must be a 1:1 agreement between the $^{14}N_2$ and $^{15}N_2$ reduction tests performed under the same conditions.

By applying our proposed protocol using isotope labelled nitrogen, we have tested several of the more promising processes and catalysts from Figure 2. Thus far, the only report we found to be reproducible was that of Tsuneto et al.'s lithium-mediated nitrogen electroreduction[24]. Using a colorimetric indophenol test and an ammonia gas sensing electrode, they measured high current densities and concentrations. Nonetheless, they lacked the crucial isotope labelled measurements. We confirmed their method yielded NH_3, using a molybdenum foil and $^{14}N_2$ gas, testing $^{14}NH_3$ with a colorimetric method and with NMR (Figure 4A). Blank tests with Ar accumulating 20 C of charge and $^{14}N_2$ gas at OCP for 1.5 hours detected no discernible amount of NH_3. Finally, we performed isotope labelling $^{15}N_2$ (containing 2% $^{14}N_2$) experiments with a gas cleaning procedure using Cu catalyst as an impurity trap (see Methods section). Isotope labelled measurement and subsequent NMR analysis confirmed electrochemical production of $^{15}NH_3$ from $^{15}N_2$, shown in Figure 4B, and the amount of accumulated ammonia correlated with the amount

of charge passed through the system. In the test with $^{14}N_2$ gas, for NMR and indophenol the mean Faradaic efficiency was respectively 6.5±1.4% and 7.5±1.1%, the mean yield rate was 0.7±0.2 μmol/h·cm^2 and 0.8±0.1 μmol/h·cm^2, and the mean concentrations measured for the 20 C measurements was 0.56±0.10 mM (9.6±1.6 ppm) and 0.65±0.08 mM (11.1±1.3 ppm). In the test with $^{15}N_2$ gas for NMR and indophenol the mean faradaic efficiency was respectively 5.7±0.7% and 7.0±2.2%, the mean yield rate was 0.6±0.1 μmol/h·cm^2 and 0.7±0.2 μmol/h·cm^2, and the mean concentration measured for the 20 C measurement was 0.49±0.05 mM (8.3±0.9 ppm) and 0.61±0.16 mM (10.3±2.7 ppm). The exact nature of the ammonia synthesis described herein will be the subject of a future report. The key point at this juncture is that ammonia can be synthesized in similar quantities both for $^{14}N_2$ and $^{15}N_2$. This set of experiments validates the suggested 'lithium-mediated' protocol for electrochemical NH_3 production, and demonstrates the use of benchmarking protocols described here.

As more systems are proven with this rigorous protocol, and the performance toward nitrogen reduction improves yielding larger amounts (orders of magnitude) of ammonia beyond the ppm range, it may not be necessary to perform quantitative isotope sensitive experiments for every measurement; the rigor of this protocol could be relaxed. The sources of contamination and suggested control experiments, while intended for electrochemical ammonia synthesis, can also be applied to photoelectrochemical experiments and for nitrogen oxidation to NO_x; the main points regarding the importance of carrying out blank tests and utilizing isotope labelled $^{15}N_2$ are still valid and should be utilized across these fields as well. A rigorous experimental benchmarking procedure will prevent false positives from appearing in the literature and help the field advance much faster towards practical, electrochemical technologies for the electoreduction of N_2 to ammonia.

References:

1. Shipman, M. A. & Symes, M. D. Recent progress towards the electrosynthesis of ammonia from sustainable resources. *Catal. Today* **286,** 57–68 (2017).

2. Jewess, M. & Crabtree, R. H. Electrocatalytic Nitrogen Fixation for Distributed Fertilizer Production? *ACS Sustain. Chem. Eng.* **4,** 5855–5858 (2016).

3. Nørskov, J., Chen, J. DOE Roundtable Report: Sustainable Ammonia Synthesis. *U.S. Dep. Energy* (2016).

4. Ye, L., Nayak-Luke, R., Bañares-Alcántara, R. & Tsang, E. Reaction: "Green" Ammonia Production. *Chem* **3,** 712–714 (2017).

5. Singh, A. R. *et al.* Electrochemical Ammonia Synthesis—The Selectivity Challenge. *ACS Catal.* **7,** 706–709 (2017).

6. Skúlason, E. *et al.* A theoretical evaluation of possible transition metal electro-catalysts for N_2 reduction. *Phys. Chem. Chem. Phys.* **14,** 1235–1245 (2012).

7. Sclafani, A., Augugliaro, V., Schiavello, M. Dinitrogen Electrochemical Reduction to Ammonia over Iron Cathode in Aqueous Medium. *J. Electrochem. Soc.* **130,** 734 (1983).

8. Zhang, Z., Zhong, Z. & Liu, R. Cathode catalysis performance of $SmBaCuMO_{5+\delta}$ (M=Fe, Co, Ni) in ammonia synthesis. *J. Rare Earths* **28,** 556–559 (2010).

9. Lan, R., Irvine, J. T. S. & Tao, S. Synthesis of ammonia directly from air and water at ambient temperature and pressure. *Sci. Rep.* **3,** 1145 (2013).

10. Dabundo, R. *et al.* The Contamination of Commercial $^{15}N_2$ Gas Stocks with ^{15}N–Labeled Nitrate and Ammonium and Consequences for Nitrogen Fixation Measurements. *PLoS One* **9,** e110335 (2014).

11. Greenlee, L. F., Renner, J. N. & Foster, S. L. The Use of Controls for Consistent and Accurate Measurements of Electrocatalytic Ammonia Synthesis from Dinitrogen. *ACS Catal.* **8,** 7820–7827 (2018).

12. Chen, G.-F. *et al.* Advances in Electrocatalytic N_2 Reduction-Strategies to Tackle the Selectivity Challenge. *Small Methods* **1800337,** 1800337 (2018).

13. Tsuneto, A., Kudo, A. & Sakata, T. Efficient Electrochemical Reduction of N_2 to NH_3 Catalyzed by Lithium. *Chem. Lett.* **22,** 851–854 (1993).

14. Montoya, J. H., Tsai, C., Vojvodic, A. & Nørskov, J. K. The Challenge of Electrochemical Ammonia Synthesis: A New Perspective on the Role of Nitrogen Scaling Relations. *ChemSusChem* **8,** 2180–2186 (2015).

15. Hager, T. *The Alchemy of Air*. (Harmony Books, 2008).

16. Boucher, D. L., Davies, J. A., Edwards, J. G. & Mennad, A. An investigation of the putative photosynthesis of ammonia on iron-doped titania and other metal oxides. *J. Photochem. Photobiol. A Chem.* **88,** 53–64 (1995).

17. Shipman, M. A. & Symes, M. D. A re-evaluation of Sn(II) phthalocyanine as a catalyst for the electrosynthesis of ammonia. *Electrochim. Acta* **258,** 618–622 (2017).

18. Shi, M.-M. *et al.* Au Sub-Nanoclusters on TiO_2 toward Highly Efficient and Selective Electrocatalyst for N_2 Conversion to NH_3 at Ambient Conditions. *Adv. Mater.* **29,** 1606550 (2017).

19. Schlesinger, W. & Hartley, A. A global budget for atmospheric NH_3. *Biogeochemistry* **15,** 191–211 (1992).

20. Turner, C., Španěl, P. & Smith, D. A longitudinal study of ammonia, acetone and propanol in the exhaled breath of 30 subjects using selected ion flow tube mass spectrometry, SIFT-MS. *Physiol. Meas.* **27,** 321–337 (2006).

21. Song, Y. *et al.* A physical catalyst for the electrolysis of nitrogen to ammonia. *Sci. Adv.* **4,** e1700336 (2018).

22. McEnaney, J. M. *et al.* Ammonia synthesis from N_2 and H_2O using a lithium cycling electrification strategy at atmospheric pressure. *Energy Environ. Sci.* **10,** 1621–1630 (2017).

23. Wang, H. *et al.* Ambient Electrosynthesis of Ammonia: Electrode Porosity and Composition Engineering. *Angew. Chemie Int. Ed.* **57,** 12360–12364 (2018).

24. Tsuneto, A., Kudo, A. & Sakata, T. Lithium-mediated electrochemical reduction of high pressure N_2 to NH_3. *J. Electroanal. Chem.* **367,** 183–188 (1994).

25. Bao, D. *et al.* Electrochemical Reduction of N_2 under Ambient Conditions for Artificial N_2 Fixation and Renewable Energy Storage Using N_2 /NH_3 Cycle. *Adv. Mater.* **29,** 1604799 (2017).

26. Chen, G.-F. *et al.* Ammonia Electrosynthesis with High Selectivity under Ambient Conditions via a Li^+ Incorporation Strategy. *J. Am. Chem. Soc.* **139,** 9771–9774 (2017).

27. Kong, J. *et al.* Electrochemical Synthesis of NH_3 at Low Temperature and Atmospheric Pressure Using a γ-Fe_2O_3 Catalyst. *ACS Sustain. Chem. Eng.* **5,** 10986–10995 (2017).

28. Yao, Y., Zhu, S., Wang, H., Li, H. & Shao, M. A Spectroscopic Study on the Nitrogen Electrochemical Reduction Reaction on Gold and Platinum Surfaces. *J. Am. Chem. Soc.* **140,** 1496–1501 (2018).

29. Kim, K., Yoo, C.-Y., Kim, J.-N., Yoon, H. C. & Han, J.-I. Electrochemical Synthesis of Ammonia from Water and Nitrogen in Ethylenediamine under Ambient Temperature and Pressure. *J. Electrochem. Soc.* **163,** F1523–F1526 (2016).

30. Zhou, F. *et al.* Electro-synthesis of ammonia from nitrogen at ambient temperature and pressure in ionic liquids. *Energy Environ. Sci.* **10,** 2516–2520 (2017).

Acknowledgement This work was supported by the Villum Foundation V-SUSTAIN grant 9455 to the Villum Center for the Science of Sustainable Fuels and Chemicals. 400 MHz and 800 MHz NMR spectra

were recorded on the spectrometers of the NMR Center at DTU supported by the Villum Foundation. We acknowledge Albert Kravos' contribution in setting up the analytical methods to detect ammonia.

Author contributions S.Z.A., V.C., S.Y., J.K., S.M., P.C.K.V., I.E.L.S., and I.C. concieved the idea for the protocol and experiment design. S.Z.A., V.C., S.M. and S.Y., performed the experiments, V.C. performed potential scale determination and iR-drop correction, S.Y. performed isotope measurements, K.E.-R. performed NMR measurements and wrote NMR section, J.S., A.C.N., and J.M.M. performed FTIR measurements and wrote FTIR section, J.K., P.C.K.V., I.E.L.S., and I.C. supervised the work, S.Z.A., V.C., and S.Y. drafted the manuscript, and all authors contributed to the editing of the manuscript.

Author information Reprints and permissions information is available at www.nature.com/reprints. The authors declare no competiting interests. Correspondence and requests for material should be addressed to I.C. (Ibchork@fysik.dtu.dk).

Figure 1. Potential range for chronoamperometric measurements (below) of pure metal catalysts and the detected amounts of ammonia in each measurement (above). Each catalyst was tested both for 1 hour and by passing 100 C of charge at -1.0, -1.5, -2.0 and -2.5 V vs RHE, where the error bars represent a change in potential during the measurement due to a changing ohmic drop correction (see Methods section).

Figure 2: An overview on literature data. Grey dots represent data without blank test, blue squares includes blank tests, red triangles represent data with $^{15}N_2$ isotope tests with blank tests, filled symbols signify non-aqueous systems, and stars are estimated values using data provided in the literature. **a** Partial current densities for electrochemical ammonia production vs. applied potential (vs. RHE unless otherwise specified). **b** Ammonia concentrations as a function of partial current density towards ammonia formation. The 10 ppb dashed line signifies the lower detection limit of ammonia in our system, and the grey gradient signifies concentrations wherein we have seen false positives (see Extended Data). **c** Faradaic efficiency of the detected ammonia as a function of partial current density towards ammonia. Data adapted from: Ref[7] for Fe; Ref[8] for SmBaCuNiO; Ref[9] for Pt; Ref[25] for Au; Ref[26] for Li^+-PEBCD (Li^+ incorporated into poly(N-

ethyl-benzene-1,2,4,5-tetracarboxylic diimide)); Ref[27] for Fe_2O_3; Ref[28] for Au; Ref[29] for Ni with a potential of 1.8 V between 2 electrodes; Ref[30] for Fe/SS with a potential vs. NHE; Ref[21] for CNS; Ref[24] for Li on Ag with a potential vs. Ag/AgCl/AgCl (sat), LiCl, $LiClO_4$/THF reference. The potential for Li on Mo in this work is -3.1 V vs. SHE.

Figure 3: Suggested protocol for the benchmarking of electrochemical nitrogen reduction.

Figure 4: Ammonia synthesised at -3.1 V and more negative potentials vs SHE (iR-drop corrected) using a Mo-cathode and Pt-anode in a 0.2 M $LiClO_4$ in 1% ethanol and 99% THF electrolyte, in the system reported by Tsuneto et al., here successful proven by repeated regular and isotope labelled experiments. **a** Representative NMR data of experiment with samples taken at 5 C, 10 C, 15 C, and 20 C using $^{14}N_2$ with THF suppression (for details see Methods section), and **b** mean and standard deviation of 3 measurements of $^{14}NH_3$ synthesized via integrated peak area from NMR data calibrated with Extended Data Figure 2B-C and indophenol. **c** Representative NMR data of experiment with $^{15}N_2$, with samples taken at 5 C, 10 C, 15 C, and 20 C, and **d** mean and standard deviation of 3 measurements of $^{15}NH_3$ synthesized via integrated peak area from NMR data calibrated with Extended Data Figure 2C-D and indophenol. The 1H spectra have been referenced setting the chemical shift of the methyl resonance from ethanol to 1.15 ppm (TMS = 0.0 ppm). Shift of NMR peaks due to slight differences in pH, volume, and/or temperature of samples.

Methods

Electrochemical measurements in aqueous electrolyte: Bio-Logic VMP2 and SP-300 (Bio-Logic, France) potentiostats were used for all electrochemical experiments. A borosilicate glass H-cell was used, with working electrode (WE) and counter electrode (CE) chambers each 7.5 ml in volume, connected by a joint separated by a membrane. The Hg-Hg_2SO_4 reference electrode (SI Analytics, Germany) reference electrode (RE) chamber is connected to the WE compartment by a glass frit. The electrolyte used is 0.1 M KOH (99.995%, Merck Suprapur®, Germany) in ultrapure water (Millipore Synergy® UV). The glassware is boiled and rinsed twice in Millipore water, then oven dried overnight at 120 °C between each measurement. We use the microporous polypropylene Celgard® 3401 membrane, with a thickness of 25 µm

and a porosity of 41% to separate WE and CE chambers. Because it is a porous membrane, as opposed to a proton or anion exchange membrane, it does not act as a source or sink for ammonia, requires no cleaning procedure, and can be kept in 0.1 M KOH. Ruthenium (6×6×1 mm^3, 99.9%, Goodfellow Inc., Canada), rhenium (10×10×2 mm^3, 99.99%, Goodfellow Inc., Canada), and rhodium (5×10×0.25 mm^3, 99.9% purity, MaTeCK, Juelich, Germany), were tested at 4 different potentials: -1.0 V, -1.5 V, -2.0 V, and -2.5 V vs. RHE, for 1 hour, or until 100 C of charge was accumulated. The CE was an iridium foil (25×25×0.125 mm^3, 99.9%, Goodfellow inc., Canada). The electrodes are polished several times using polycrystalline diamond paste (Buehler, USA) respectively of sizes 3 µm, 1 µm, and 0.25 µm, until the surface has a mirror finish, followed by an ultra-sonication process in Millipore water and isopropanol (≥ 99.8%, Merck, Germany) between each polishing step, to dislodge any remaining diamond particles. The WE's were annealed at 700-800 ^oC by induction heating with Ar/5%-H_2 (AGA Gas AB, Sweden) atmosphere for 5 minutes. Given the generally low Faradaic efficiencies observed for nitrogen reduction in the literature, we applied relatively high currents (10-50 mA) to maximise the ammonia in the system. The Ohmic resistance was measured at OCP, by conducting EIS spectra from 30 kHz to 1 Hz before and after each measurement, fitted using EC-Lab V11.02. A shunt capacitance of 2 µF was connected between the RE and CE to eliminate high-frequency artefacts. Bubble formation during the measurement would result in additional uncorrected Ohmic drops. The EIS spectra were fitted using the software to determine the uncompensated resistance. The iR-drop correction was carried out taking into account the current flowing at the given potential. Measurements were conducted with an 85% *iR*-drop automatic compensation, based on the pre-test resistance; the remaining 15% *iR*-drop was corrected a posterior. The pre-test Ohmic drop was higher than the post-test value, due to rising electrolyte levels in the WE compartment and temperature increases; we thus represent the potential as a range of values to account for this change in potentials. Additionally, when we attempted to measure the Ohmic drop in operando, we measured additional at least 6% increase relative to the OCP, due to bubble formation;[31] typically such in operando measurements were impractical, due to the potentiostat overloading. Thus, in order to account for uncertainty in the Ohmic drop, we represent it is a range of values, rather than a discrete datapoint. The higher hydrogen evolution activity of Rh at very

negative potentials resulted in particularly large difference between the pre-test and post-test Ohmic drop value, manifested as a large uncertainty in potential.

Figure 1 displays the potential measured for each metal during CA. All of the pure metal catalysts resulted in <10 ppb NH_3, detected via the colorimetric indophenol method at the measured potentials, within the levels of background contamination of the setup. These catalysts show much higher selectivity towards the competing HER in aqueous solutions, consistent with DFT-based models[14].

Electrochemical measurements in non-aqueous electrolyte: The experiments were performed in an OMNI-LAB (Vacuum Atmospheres Co., USA) glovebox and a home-made closed system with N_2 gas recirculation. The single compartment borosilicate glass cell had an electrolyte volume of 8 ml. It had a two-electrode configuration with a Mo foil (0.125 mm, 99.9%, Goodfellow, UK) WE and a Pt-mesh (99.9%, Goodfellow, UK) CE. Experiments in non-aqueous electrolytes were conducted in 0.2 M $LiClO_4$ (battery grade, 99.99%, Sigma Aldrich, Germany) in a mixture of 1 vol.% ethanol (99.5%, AcroSeal®, Sigma Aldrich, Germany) and 99 vol.% tetrahydrofuran (THF, anhydrous, 99.9%, inhibitor-free, Sigma Aldrich). The exact potential vs. SHE was difficult to determine due to the large Ohmic drop and fluctuating current. It was estimated in a three-electrode system using a Ag/Ag^+ electrode prepared by immersing a silver wire (Dansk Hollandsk Ædelmetal, Denmark) in a 0.1 M $AgClO_4$ (Sigma Aldrich, Denmark) in THF, separated from the main chamber with a P4 glass frit. The potential of this electrode was calculated to be 0.77 V vs. SHE using data from Gritzner[32]. The Ohmic drop was measured by the means of EIS. It was generally in the range of 900-1600 Ω for the 0.2 M solution of $LiClO_4$. For the catalytic tests, a bias of –9 V was applied between the electrodes; the current which was in the range of 2-3 mA. Using this system, we estimate the initial WE potential to be ~-3.1 V under reaction conditions, which became more negative during the experiment.

Colorimetric tests to determine concentration of ammonia, nitrite, and hydrazine: Ammonia in the electrolyte was quantified by the indophenol method, which works well for aqueous electrolytes and can be modified to work for non-aqueous electrolytes. For calibration in aqueous electrolytes, a known concentration of NH_4Cl (99.8%, Merck) was added to 0.1 M KOH, then neutralized by adding 0.5 M H_2SO_4 (Suprapur, Merck, Germany). 500 µl of phenol nitroprusside solution (P6994, Sigma Aldrich) and 500 µl of alkaline hypochlorite solution (A1727, Sigma Aldrich) was then added to 2 ml of the neutralized sample. The solution was incubated for 30 min at room temperature in the dark, and the sample absorbance was analyzed by UV-vis spectrometer (UV-2600, Shimadzu, Japan) from 400 nm to 800 nm. The calibration curve was constructed for ammonia with the following concentrations: blank, 10 ppb, 50 ppb, 100 ppb, 500 ppb, 1 ppm and 2 ppm, and a fitted curve of the absorbance peak of each concentration showed a linear regression with an R-squared value of 0.99965. For the non-aqueous electrolyte (0.2 M $LiClO_4$ in 1% ethanol/99% THF), 20 µl of 4 M HCl (37%, VWR Chemicals, USA) was added to 400 µl of the electrolyte, and the solution was dried at 60 ºC for 30 min, evaporating the solvent while leaving ammonia in the form of NH_4Cl salt. The remaining salts were dissolved in 2 ml of Milli-Q H_2O, and the indophenol method proceeded as described for the aqueous case. The calibration curve was constructed for ammonia with the same concentrations as the aqueous case, and a fitted curve of the absorbance peak of each concentration showed a linear regression with an R-squared value of 0.99737. It is imperative to make a blank measurement for every sample using the same batch of chemicals, which ensures no significant contamination of the chemicals.

NO_x contamination is often present in N_2 gas bottles. NO_x can be reduced to ammonia much more easily than N_2; consequently, since its presence could lead to a false positive, it is important to account for it. Nitrite, NO_2^-, can easily be detected down to 10 ppb with colorimetric tests. For the aqueous electrolyte, a known concentration of KNO_2 (≥ 96.0%, Sigma Aldrich) was added to 0.1 M KOH, then neutralized by adding 0.5 M H_2SO_4. Subsequently 35 mg of powder was added from a nitrite test kit (photometric 0.002-1.00 mg/l NO_2-N 0.007 - 3.28 mg/l NO_2^- Spectroquant®, Merck, Germany), containing sulfanilic acid and diazonium salt, to 3 ml of the neutralized solution. This was incubated for 10 min at room temperature

before being analyzed by UV-vis spectrometry. A calibration curve was constructed with the same nitrite concentrations as the ammonia calibration; the fitted curve for the calibration showed a linear regression with an R-squared value of 0.99933.

Hydrazine can potentially be produced during ammonia synthesis. For the aqueous electrolyte, a known concentration of hydrazine monohydrate (~64%, Sigma Aldrich) was added to 0.1 M KOH, then neutralized by adding 0.5 M H_2SO_4. This was followed by adding 1 ml of the reagent solution from the hydrazine test kit (photometric 0.005 - 2.00 mg/l N_2H_4 Spectroquant®, Merck, Germany), containing 4-(dimethylamino)benzaldehyde, to 2.5 ml of the neutralized solution, and the new solution was incubated for 5 min at room temperature, before being analyzed by UV-vis spectrometry. A calibration curve was constructed with the same hydrazine concentrations as the ammonia calibration; the fitted curve for the calibration showed a linear regression with an R-squared value of 0.99999.

Single compartment cells have the advantage of removing one parameter of possible ammonia contamination: the membrane. The single-compartment cell used in this work consisted of a clean glass cell containing 5 ml 0.1 M KOH electrolyte, with Ru as WE and Ir as CE, using a glass bubbler to saturate the electrolyte with N_2 gas. However, when we added 1 ppm of ammonia to such a setup in order to evaluate the efficiency of ammonia retrieval, using Ar gas (5.0, AGA Gas AB, Sweden) instead of N_2 (to exclude contamination from the gas stream), and applied potentials around -2.5 V vs. RHE for 1 hour, only 46 ppb and 54 ppb of the added ammonia could be recovered in two separate experiments. Ammonia was removed from the electrolyte, either by hydrogen bubble formation at the WE or by oxidation at the CE.

An acid or water trap downstream of the electrochemical cell is often used to capture gas phase ammonia. However, due to the high solubility of ammonia in water, it tends to remain in aqueous electrolytes even at very high pH-values[33]. Therefore, one must evaluate the need for a downstream trap, as it is potentially redundant. Moreover, such a downstream trap could also be a serious source of contamination between experiments. We have not implemented a downstream trap.

Nafion is a commonly used membrane and binder. In order to assess the influence of a Nafion membrane, we conducted a series of measurements in the two-compartment cell with 7.5 ml 0.1 M KOH as electrolyte, Ru as WE and Ir as CE, both with the "as-used" working electrolyte and after adding a set amount of ammonia. The Nafion (Nafion 117, Chemours) was either used as received, or pre-cleaned by boiling it for 1 hour in 3% H_2O_2 (30%, Merck, Germany), boiling it for 1 hour in 0.1 M H_2SO_4, and then rinsing in Millipore water to remove excess acid. We observed a reduction in the concentration of ammonia in 0.1 M KOH solutions in contact with fresh Nafion. This is due to the membrane soaking up background contamination of ammonia from the electrolyte it is submerged in, relative to a blank sample from the same batch of 0.1 M KOH, which had not been in contact with Nafion. This leads to a "negative" concentration relative to the blank, as shown in Extended Data Figure 1A. On the other hand, when the Nafion is pre-cleaned using the aforementioned method, the membrane becomes a source of ammonia contamination. The membrane likely absorbs ammonia from the acid during cleaning, which is later released. Moreover, with no applied potential, the membrane allows for significant crossover of ammonia from the WE compartment to the CE compartment (1 ppm added to WE, recovered 945 ppb in WE and 178 ppb in CE after 1 hour). With applied potential the ammonia from the CE compartment becomes negative (1 ppm added to WE, recovered 925 ppb in WE and -20 ppb in CE after 1 hour at -0.5 V vs RHE with Ar), most likely due to a combination of oxidization at the CE and absorption into the membrane. Since Nafion can both be sink or source of ammonia, it should be used with great care in ammonia synthesis.

Celgard®: The Celgard 3401 membrane is a 25 µm thick microporous polypropylene membrane. No significant increase or decrease in the detected levels of adventitious ammonia is measured with this membrane, shown in Extended Data Figure 1B. When 1 ppm of ammonia is added to the working electrode compartment at OCP, all of the ammonia was recovered. With an applied potential of -2.5 V vs RHE using Ar gas, crossover across the membrane increases, and 791 ppb of the 1 ppm of ammonia added was recovered from the WE compartment, and 89 ppb was recovered at the CE compartment. An H-cell with the Celgard membrane was therefore used for all aqueous experiments.

Additional sources of contamination: Three clean glass vials separately containing 2 ml 0.1 M KOH, 2 ml Millipore H_2O, and 2 ml 0.1 M $HClO_4$ were left open in the laboratory. After 24 hours, they contained significant amounts of ammonia, as shown in Extended Data Figure 1C, repeated three times on different days. To show the possible contamination from human breath, an experiment in which one participant exhaled 3 L (close to the average human full-breath capacity) through a glass tube inserted into 2 ml of 0.1 M KOH was conducted and repeated in 3 measurements. Extended Data Figure 1D shows that the amount of ammonia accumulated in this manner can be significant. Additionally, nitrile rubber gloves are commonly used in laboratory work. Nitrile rubber is a copolymer of acrylonitrile and butadiene. Acrylonitrile is typically produced by catalytic ammoxidation of propylene, where ammonia is used as a reactant. We sonicated a ~ 5 cm^2 of a nitrile glove (Pharma und Kosmetik GmbH, Germany) in 10 ml DI-water for 1 h, and 2.8 ppm was detected by the indophenol method. Care must therefore be taken when using nitrile gloves in ammonia synthesis.

We stress that the contamination levels that we observed herein are not definitive: they depend on cleaning procedures and environmental factors like ambient ammonia concentration. Nonetheless our experiments provide examples of how contamination in a given set-up can be quantified.

Mass spectrometry (MS). Isotope labelled ammonia can be detected via MS ue to the atomic weight difference between $^{14}NH_3$ and $^{15}NH_3$. Unfortunately, H_2O has a mass difference of only 0.008 amu compared isotope labelled $^{15}NH_3$, so suppression of the water signal, e.g. by lowering the ionization potential coupled with very high resolution, could quantify the $^{15}NH_3$ signal. Other strategies to mitigate the interference from water have thus far only yielded qualitative data[21].

Gas phase FTIR spectroscopy. FTIR can distinguish between $^{14}NH_3$ and $^{15}NH_3$, based on the atomic mass difference and the corresponding change to the vibrational frequencies. This manifests itself as a roughly 5 wavenumber shift in the wagging mode of ammonia (see Extended Data Figure 3) centered around 940 wavenumbers, in accordance with the prediction of the quantum mechanical harmonic oscillator[22].

Nuclear magnetic resonance (NMR) spectroscopy. All NMR experiments were performed at 25 °C on a Bruker AVANCEIII HD spectrometer operating at a ^{1}H frequency of 800.182 MHz and equipped with a 5mm TCI CryoProbe (Bruker Biospin) or a Bruker AVANCE III HD spectrometer operating at a ^{1}H frequency of 400.13 MHz equipped with a Prodigy probe (Bruker Biospin). One way to confirm the successful electrochemical production of NH_3 from isotope labelled $^{15}N_2$ experiments could be a standard "pulse and acquire" NMR experiment tuned to the resonance frequency of ^{15}N. Despite using a ^{15}N-labeled precursor, the low production yield, coupled with unfavorable NMR properties of ^{15}N (e.g. low gyromagnetic ratio and long T1 relaxation constants) limits the sensitivity of ^{15}N for this application. ^{1}H NMR is the better choice for sensitivity, as it can differentiate $^{15}NH_4^+$ from $^{14}NH_4^+$, since ^{14}N is a spin-1 nucleus and ^{15}N is a spin-½ nucleus. Consequently, the scalar interaction between ^{1}H and ^{15}N in $^{15}NH_4^+$ results in a splitting of the ^{1}H resonance into two symmetric signals, with a spacing of 73 Hz; the magnitude of the ^{1}H-^{15}N scalar interaction. On the other hand, the ^{1}H resonance for ^{1}H coupled to ^{14}N in $^{14}NH_4^+$ is split into three symmetric signals with a spacing of 52 Hz. For the samples prepared in H_2O the water resonance was suppressed with the excitation sculpting method using a 3 ms 180° shaped pulse centered at 4.70 ppm. The perfect-echo variant was chosen to reduce J- modulation for the samples analyzed at 800 MHz. A total of 1024 transient scans were recorded with an inter-scan delay of 1 second. 64K complex points was acquired for each FID with an acquisition time of 3.4 seconds. The processed spectra have been zero-filled to 64K real points and an exponential apodization function with lb = 0.3 Hz was applied prior to Fourier transformation (FT). 3 vol.% D_2O (99.9%, Sigma Aldrich, Denmark) was added for deuterium locking and referencing. For the samples analyzed at 400 MHz it was necessary to add 10 vol.% D_2O for sufficient lock signal. For the samples prepared in THF/ethanol the 1D-NOESY pre-saturation method was utilized to suppress the two THF signals. A train of 100 ms square pulses centered at 3.66 ppm with a frequency modulation of 1.82 ppm was applied during the relaxation delay (3 seconds) and mixing time (100 ms). ^{13}C cw-decoupling was applied during the acquisition time to decrease the intensity of the THF satellite signals. A total of 512 transient scans were recorded. 16K complex points was acquired for each FID with an acquisition time of 3.4 seconds. Linear prediction was used to double the number of complex points and

the FID was subsequently zero-filled to 32K real points. An exponential apodization function with lb = 1Hz was applied prior to FT. 5 vol.% THF-d8 (99.9%, Sigma Aldrich, Denmark) was added for deuterium locking and referencing. Calibration samples were prepared with varying concentrations of $^{14}NH_4Cl$ (99.8%, Merck, Germany) and $^{15}NH_4Cl$ (98 atom% ^{15}N, Sigma Aldrich, Denmark).

Gas circulation setup for isotope measurements: While we stress the importance of isotope labelling experiments, we acknowledge the high price and small volume of $^{15}N_2$ gas bottles makes such measurements challenging. Furthermore, the low activity of the nitrogen reduction reaction requires the experiment to run for an extended time, with a continuous supply of N_2 gas. Typically, a few litres or tens of litres are required for each measurement, and most of the gas is lost as exhaust. Nevertheless, the price of USD 2,100 for 5 liters 98% $^{15}N_2$ is nothing compared to having an incorrect scientific report published, which potentially can mislead the entire field. Therefore, we designed a circulation setup where $^{15}N_2$ gas was continuously cycled and re-supplied to the electrode surface. A simplified schematic and picture of our setup is shown in Extended Data Figure 4. A 4-way valve is central to the set-up, and enables the choice between purging mode, i.e. gas flowing through the entire set-up to the exhaust, and circulating mode, i.e. gas being cycled in the enclosed system by a pump. The volume of the enclosed cycling system is about 100 ml (4.46 mmol N_2), which for the present conversion range is plenty. The inlet gas passes through a Cu impurity trap and a cold trap, described in detail in the following section, to remove any impurity supplied to the system. A water trap before the exhaust limits the possibility of back flow. Before flowing $^{15}N_2$ gas, Ar gas is first flowed through the whole set-up for 30 min to remove any $^{14}N_2$ gas that was present in the system. After sufficient purging with Ar, $^{15}N_2$ is flowed for 20 min with a flow rate of 10 ml min^{-1}. Then the 4-way valve is switched to circulating mode, and the isotope experiments were performed. $^{14}N_2$ experiments were performed in the exactly the same manner, except for the unnecessary Ar purging beforehand. The setup also allows the flow of 10% H_2 in Ar through the gas line that is used for the activation of the copper catalyst.

Cleaning of $^{15}N_2$ gas: Cleaning of the $^{15}N_2$ gas (98 atom% ^{15}N, Sigma Aldrich) is very important, since $^{15}N_2$ may contain significant impurities, in the form of $^{15}NH_3$ along with $^{15}NO_x$ species[10]. We tested the purity of our $^{15}N_2$ by first saturating our solution of 0.1 M KOH with Ar to remove any excess $^{14}N_2$, followed by bubbling ~ 200 ml of $^{15}N_2$. We circulated the 200 ml $^{15}N_2$ gas for 1 h to duplicate the long-term electrochemical measurement. The resulting solution was analyzed via colorimetric tests to detect NH_3, NO_2^-, and N_2H_4 and NMR to differentiate $^{14}NH_4^+$ from $^{15}NH_4^+$. With NMR spectroscopy, shown in Extended Data Figure 5, we observed a detectable amount of $^{14}NH_4^+$, which is as an unavoidable impurity. However, we could not observe any $^{15}NH_4^+$ species. Colorimetric tests also confirmed <10 ppb of NH_3 in the solution, seen in Extended Data Figure 6A. Given the result, we concluded that $^{15}NH_3$ contamination for our system is negligible. Unlike ammonia, we clearly observed >10 ppb of nitrite from the colorimetric test, as seen Extended Data Figure 6C. NO_2^- can easily be reduced to NH_4^+ and would give a false positive, even in the isotope labelled tests. To remove these impurities, a Cu impurity trap was introduced, composed of 2 g Cu-Zn-Al oxide catalyst in a U shaped stainless steel tubing[34,35]. The Cu catalyst was reduced before each experiment in a 5% H_2/Ar stream at 300 °C for 2 hours. The gas flow was switched to Ar at 300 °C for 30 min, and the Cu impurity trap was cooled down to –100 °C using an ethanol slurry, prepared by mixing ethanol with liquid nitrogen. Ar flow through the Cu impurity trap was used to purge out the entire system for 30 min, including the gas tight electrochemical cell. The electrolyte was then injected using a syringe to the Ar purged electrochemical cell to prevent exposure to air and moisture. Ar was bubbled through the electrolyte for an additional 30 min to remove dissolved $^{14}N_2$. Finally, $^{15}N_2$ was introduced to the electrochemical system through the reduced Cu impurity trap. After bubbling $^{15}N_2$ gas for 15 min (~200 ml), the gas was circulated in a closed loop using a glass pump (Makuhari Rikagaku Garasu Inc., Japan). Using this cleaning procedure, three repeated measurements were carried out. The first test with the cleaning procedure showed up to 25 ppb of ammonia, as seen in Extended Data Figure 6B. We assume this to be due to leftover contamination of the catalyst, or unaccounted impurity from the environment. Both, however, were in the form of $^{14}NH_4^+$ as seen with NMR, and should therefore not interfere with the isotope labelling measurements. For the 2nd and 3rd tests with the cleaning procedure, no ammonia was detected.

For nitrite measurements, small amounts of nitrite in the gas stream was clearly removed, and we could not detect any nitrite after the cleaning procedure, as seen in Extended Data Figure 6D. No hydrazine was measured before the cleaning procedure as seen in Extended Data Figure E. Such a cleaning procedure is important to definitively prove the catalytic conversion from $^{15}N_2$ to $^{15}NH_3$. Other techniques may be utilized to clean the $^{15}N_2$ gas, such as using a commercial gas purifier (MicroTorr MC1-902F, SAES Pure Gas), with certified < 5 pptV of NH_3 and < 1 pptV of NO_X impurities.

31. Čolić, V. *et al.* Experimental Aspects in Benchmarking of the Electrocatalytic Activity. *ChemElectroChem* **2,** 143–149 (2015).

32. Gritzner, G. Standard electrode potentials of $M^+|M$ couples in non-aqueous solvents (molecular liquids). *J. Mol. Liq.* **156,** 103–108 (2010).

33. Brass, M., Pritzel, T., Schulte, E., and Keller, J.U. Measurements of Vapor-Liquid Equilibria in the Systems NH_3-H_2O-NaOH and NH_3-H_2O-KOH at Temperatures of 303 and 318 K and Pressures 0.1 MPa<p<1.3 MPa. *Int. J. Thermophys.* **21,** 883–898 (200AD).

34. Ma, L. *et al.* In situ DRIFTS and temperature-programmed technology study on NH_3-SCR of NO_x over Cu-SSZ-13 and Cu-SAPO-34 catalysts. *Appl. Catal. B Environ.* **156–157,** 428–437 (2014).

35. Ma, L. *et al.* Characterization of commercial Cu-SSZ-13 and Cu-SAPO-34 catalysts with hydrothermal treatment for NH_3-SCR of NO_x in diesel exhaust. *Chem. Eng. J.* **225,** 323–330 (2013).

36. Cook, R. L. & Sammells, A. F. Ambient temperature gas phase electrochemical nitrogen reduction to ammonia at ruthenium/solid polymer electrolyte interface. *Catal. Letters* **1,** 345–349 (1988).

37. Furuya, N. & Yoshiba, H. Electroreduction of nitrogen to ammonia on gas-diffusion electrodes modified by Fe-phthalocyanine. *J. Electroanal. Chem. Interfacial Electrochem.* **263,** 171–174

(1989).

38. Furuya, N. & Matsui, K. Electroreduction of carbon dioxide on gas-diffusion electrodes modified by metal phthalocyanines. *J. Electroanal. Chem. Interfacial Electrochem.* **271,** 181–191 (1989).

39. Kordali, V., Kyriacou, G. & Lambrou, C. Electrochemical synthesis of ammonia at atmospheric pressure and low temperature in a solid polymer electrolyte cell. *Chem. Commun.* 1673–1674 (2000). doi:10.1039/b004885m

40. Pospíšil, L. *et al.* Electrochemical conversion of dinitrogen to ammonia mediated by a complex of fullerene C_{60} and γ-cyclodextrin. *Chem. Commun.* 2270–2272 (2007). doi:10.1039/B701017F

41. Xu, G., Liu, R. & Wang, J. Electrochemical synthesis of ammonia using a cell with a Nafion membrane and $SmFe_{0.7}Cu_{0.3-x}Ni_xO_3$ (x = 0−0.3) cathode at atmospheric pressure and lower temperature. *Sci. China Ser. B Chem.* **52,** 1171–1175 (2009).

42. Kugler, K., Luhn, M., Schramm, J. A., Rahimi, K. & Wessling, M. Galvanic deposition of Rh and Ru on randomly structured Ti felts for the electrochemical NH_3 synthesis. *Phys. Chem. Chem. Phys.* **17,** 3768–3782 (2015).

43. Li, S.-J. *et al.* Amorphizing of Au Nanoparticles by CeO_x -RGO Hybrid Support towards Highly Efficient Electrocatalyst for N_2 Reduction under Ambient Conditions. *Adv. Mater.* **29,** 1700001 (2017).

44. Chen, S. *et al.* Electrocatalytic Synthesis of Ammonia at Room Temperature and Atmospheric Pressure from Water and Nitrogen on a Carbon-Nanotube-Based Electrocatalyst. *Angew. Chemie Int. Ed.* **56,** 2699–2703 (2017).

45. Marnellos, G. Ammonia Synthesis at Atmospheric Pressure. *Science (80-.).* **282,** 98–100 (1998).

46. Murakami, T., Nohira, T., Goto, T., Ogata, Y. H. & Ito, Y. Electrolytic ammonia synthesis from water and nitrogen gas in molten salt under atmospheric pressure. *Electrochim. Acta* **50,** 5423–

5426 (2005).

47. Wang, B. H., Wang, J. De, Liu, R., Xie, Y. H. & Li, Z. J. Synthesis of ammonia from natural gas at atmospheric pressure with doped ceria–$Ca_3(PO_4)_2$–K_3PO_4 composite electrolyte and its proton conductivity at intermediate temperature. *J. Solid State Electrochem.* **11,** 27–31 (2006).

48. Köleli, F. & Kayan, D. B. Low overpotential reduction of dinitrogen to ammonia in aqueous media. *J. Electroanal. Chem.* **638,** 119–122 (2010).

49. Amar, I. A. *et al.* Electrochemical synthesis of ammonia based on doped-ceria-carbonate composite electrolyte and perovskite cathode. *Solid State Ionics* **201,** 94–100 (2011).

50. Amar, I. A., Lan, R., Petit, C. T. G., Arrighi, V. & Tao, S. Electrochemical synthesis of ammonia based on a carbonate-oxide composite electrolyte. *Solid State Ionics* **182,** 133–138 (2011).

51. Amar, I. A. *et al.* Electrochemical synthesis of ammonia from N_2 and H_2O based on $(Li,Na,K)_2CO_3$–$Ce_{0.8}Gd_{0.18}Ca_{0.02}O_{2-\delta}$ composite electrolyte and $CoFe_2O_4$ cathode. *Int. J. Hydrogen Energy* **39,** 4322–4330 (2014).

52. Licht, S. *et al.* Ammonia synthesis by N_2 and steam electrolysis in molten hydroxide suspensions of nanoscale Fe_2O_3. *Science (80-.).* **345,** 637–640 (2014).

53. Lan, R., Alkhazmi, K. A., Amar, I. A. & Tao, S. Synthesis of ammonia directly from wet air at intermediate temperature. *Appl. Catal. B Environ.* **152–153,** 212–217 (2014).

54. Amar, I. A., Lan, R. & Tao, S. Electrochemical Synthesis of Ammonia Directly from Wet N_2 Using $La_{0.6}Sr_{0.4}Fe_{0.8}Cu_{0.2}O_{3-\delta}$-$Ce_{0.8}Gd_{0.18}Ca_{0.02}O_{2-\delta}$ Composite Catalyst. *J. Electrochem. Soc.* **161,** H350–H354 (2014).

55. Amar, I. A., Lan, R., Petit, C. T. G. & Tao, S. Electrochemical Synthesis of Ammonia Based on Co_3Mo_3N Catalyst and $LiAlO_2$–$(Li,Na,K)_2CO_3$ Composite Electrolyte. *Electrocatalysis* **6,** 286–294 (2015).

56. Cui, B. *et al.* Electrochemical synthesis of ammonia directly from N_2 and water over iron-based catalysts supported on activated carbon. *Green Chem.* **19,** 298–304 (2017).

57. Van Tamelen, E. E. & Akermark, B. Electrolytic reduction of molecular nitrogen. *J. Am. Chem. Soc.* **90,** 4492–4493 (1968).

58. Becker, J. Y., Avraham (Tsarfaty), S. & Posin, B. Nitrogen fixation: Electrochemical reduction of titanium compounds in the presence of catechol and N_2 in MeOH or THF. *J. Electroanal. Chem. Interfacial Electrochem.* **230,** 143–153 (1987).

59. Köleli, F. & Röpke, T. Electrochemical hydrogenation of dinitrogen to ammonia on a polyaniline electrode. *Appl. Catal. B Environ.* **62,** 306–310 (2006).

60. Kim, K. *et al.* Communication—Electrochemical Reduction of Nitrogen to Ammonia in 2-Propanol under Ambient Temperature and Pressure. *J. Electrochem. Soc.* **163,** F610–F612 (2016).

61. Zhu, D., Zhang, L., Ruther, R. E. & Hamers, R. J. Photo-illuminated diamond as a solid-state source of solvated electrons in water for nitrogen reduction. *Nat. Mater.* **12,** 836–841 (2013).

62. Dong, G., Ho, W. & Wang, C. Selective photocatalytic N_2 fixation dependent on g-C_3N_4 induced by nitrogen vacancies. *J. Mater. Chem. A* **3,** 23435–23441 (2015).

63. Banerjee, A. *et al.* Photochemical Nitrogen Conversion to Ammonia in Ambient Conditions with FeMoS-Chalcogels. *J. Am. Chem. Soc.* **137,** 2030–2034 (2015).

64. Li, J., Li, H., Zhan, G. & Zhang, L. Solar Water Splitting and Nitrogen Fixation with Layered Bismuth Oxyhalides. *Acc. Chem. Res.* **50,** 112–121 (2017).

65. Liu, J. *et al.* Nitrogenase-mimic iron-containing chalcogels for photochemical reduction of dinitrogen to ammonia. *Proc. Natl. Acad. Sci.* **113,** 5530–5535 (2016).

66. Hu, S. *et al.* Effect of Cu(I)–N Active Sites on the N_2 Photofixation Ability over Flowerlike

Copper-Doped g-C_3N_4 Prepared via a Novel Molten Salt-Assisted Microwave Process: The Experimental and Density Functional Theory Simulation Analysis. *ACS Sustain. Chem. Eng.* **5,** 6863–6872 (2017).

67. Hirakawa, H., Hashimoto, M., Shiraishi, Y. & Hirai, T. Photocatalytic Conversion of Nitrogen to Ammonia with Water on Surface Oxygen Vacancies of Titanium Dioxide. *J. Am. Chem. Soc.* **139,** 10929–10936 (2017).

Extended Data

Extended Data Table 1. Literature data on electrochemical N_2 reduction to ammonia in near-ambient condition. Ambient conditions were noted as 25 °C. All pressures were ambient. No reported TOF.

* denotes calculated (or estimated) concentrations from parameters given in the papers.

Extended Data Table 2. Electrochemical N_2 reduction to ammonia at high temperature or pressure. Ambient conditions were noted as 25 °C and 1 atm. No reported TOF.

* denotes calculated (or estimated) concentrations from parameters given in the papers.

Extended Data Table 3. Electrochemical N_2 reduction to ammonia in non-aqueous electrolyte. Ambient conditions were noted as 25 °C and 1 atm. No reported TOF.

* denotes calculated (or estimated) concentrations from parameters given in the papers.

Extended Data Table 4. Photochemical N_2 reduction to ammonia in non-aqueous electrolyte. Values in blue color are calculated (or estimated) with given values in the papers. Ambient conditions were 25°C and 1 atm.

* denotes calculated (or estimated) rate and concentration from parameters given in the papers.

Extended Data Figure 1. Concentrations of ammonia produced by various possible contamination sources. All measurements are repeated 3 times, displaying the mean and standard deviation. a) New and treated

Nafion membranes, b) New Celgard membrane, c) Leaving 2 ml of 0.1 M solutions or MilliQ H_2O open overnight, d) One person breathing 3L air through a glass straw into 2 ml 0.1 M KOH.

Extended Data Figure 2. NMR data acquired with a Bruker Avance III HD 800 MHz spectrometer equipped with a 5 mm TCI CryoProbe. Solutions contain equal concentrations of $^{14}NH_4^+$ and $^{15}NH_4^+$ from NH_4Cl. **a** Solution of 600 µl 0.1M KOH, acidified with 0.5 M H_2SO_4 to a pH of 1. 200 µM CH_3OH added as internal reference. **b** Integrated peak area from **a** for both $^{14}NH_4$ and $^{15}NH_4$. **c** Solution of 500 µl 0.1 M $LiClO_4$ in THF and ethanol with a ratio of 99:1, respectively with 2 µl 4M HCl and 50 µl d-THF. **d** Integrated peak area from **c** for both $^{14}NH_4$ and $^{15}NH_4$. Variation of chemical shift of NMR peaks is due to slight differences in pH, volume, and/or temperature of samples. **e** Zoom of lower concentrations from **a**. **f** Same concentrations and solution as **a**, using Bruker AVANCE III HD 400 MHz spectrometer equipped with a 5 mm Prodigy probe.

Extended Data Figure 3. Gas phase FTIR spectra of labelled and unlabeled ammonia acquired on a Nicolet iS50 spectrometer fitted with a 2m path length gas cell heated to 135°C. Total volume of vaporized sample is 100 µl. Ammonia concentration was 1000 ppm in H_2O prior to vaporization.

Extended Data Figure 4. The setup for gas ($^{15}N_2$, $^{14}N_2$, Ar, or 10% H_2 in Ar) circulation through the electrochemical cell (A) schematics of the setup (B) photograph of the setup with the components denoted. The pump that circulates the gas through the setup is situated behind the metal panel, and its position is outlined by the white dashed rectangle.

Extended Data Figure 5. The 1H NMR spectra of the samples after purging the solution with $^{15}N_2$ gas using Bruker AVANCE III HD 800 MHz spectrometer equipped with a 5 mm TCI CryoProbe. No $^{15}NH_4^+$ was seen in the measurements.

Extended Data Figure 6. Three sequentially repeated concentration measurements of: **a** ammonia via indophenol without cleaning the gas stream, **b** ammonia via indophenol with the applied cleaning

procedure, **c** nitrite concentration without cleaning the gas stream, **d** nitrite concentration with the applied cleaning procedure, and **e** hydrazine concentration without cleaning the gas stream.

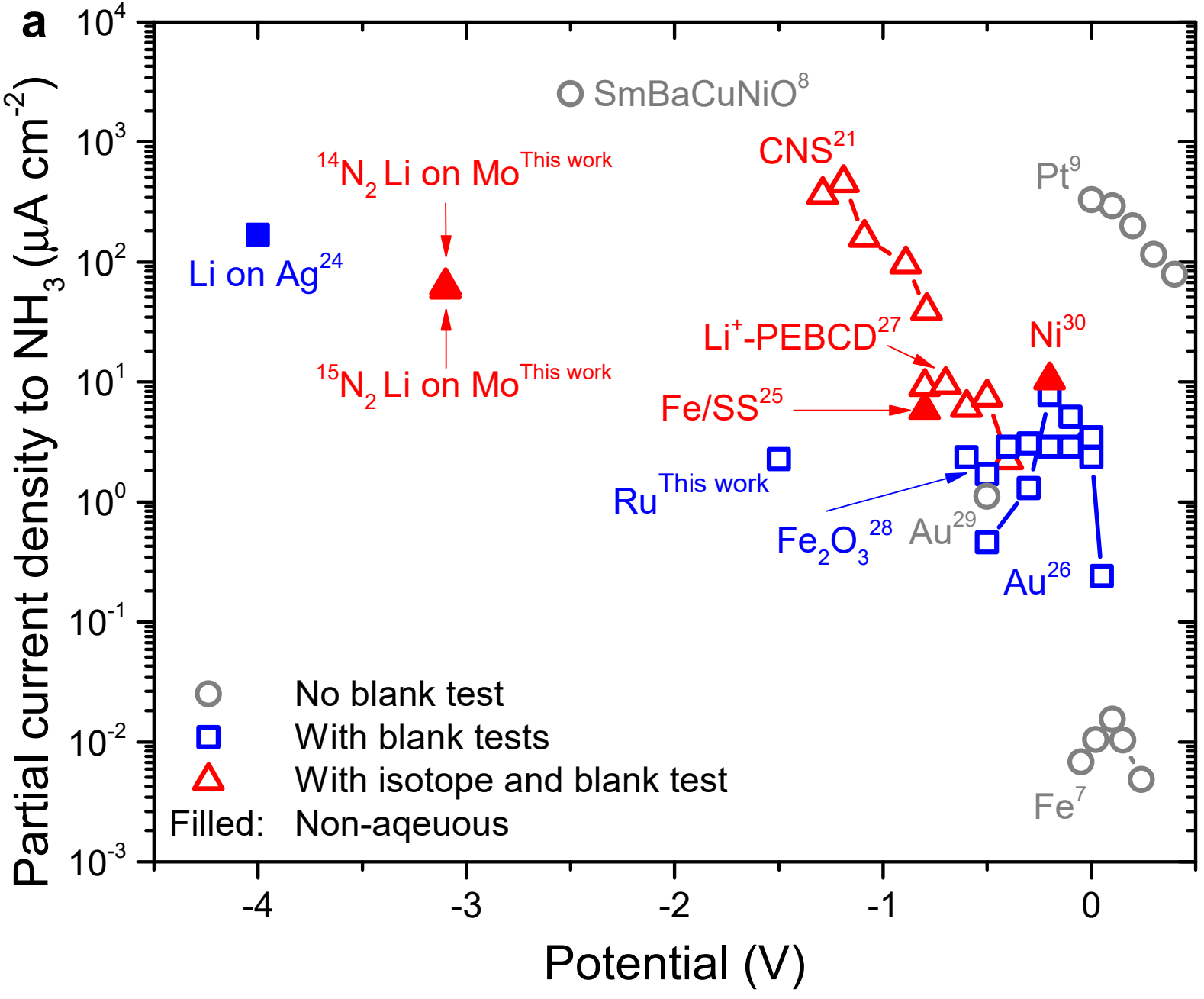
a
Partial current density to NH3 (μA cm-2)
Potential (V)
SmBaCuNiO8
14N2 Li on Mo This work
15N2 Li on Mo This work
Li on Ag24
CNS21
Pt9
Li+-PEBCD27
Ni30
Fe/SS25
Ru This work
Fe2O3 28
Au29
Au26
Fe7
No blank test
With blank tests
With isotope and blank test
Filled: Non-aqeuous

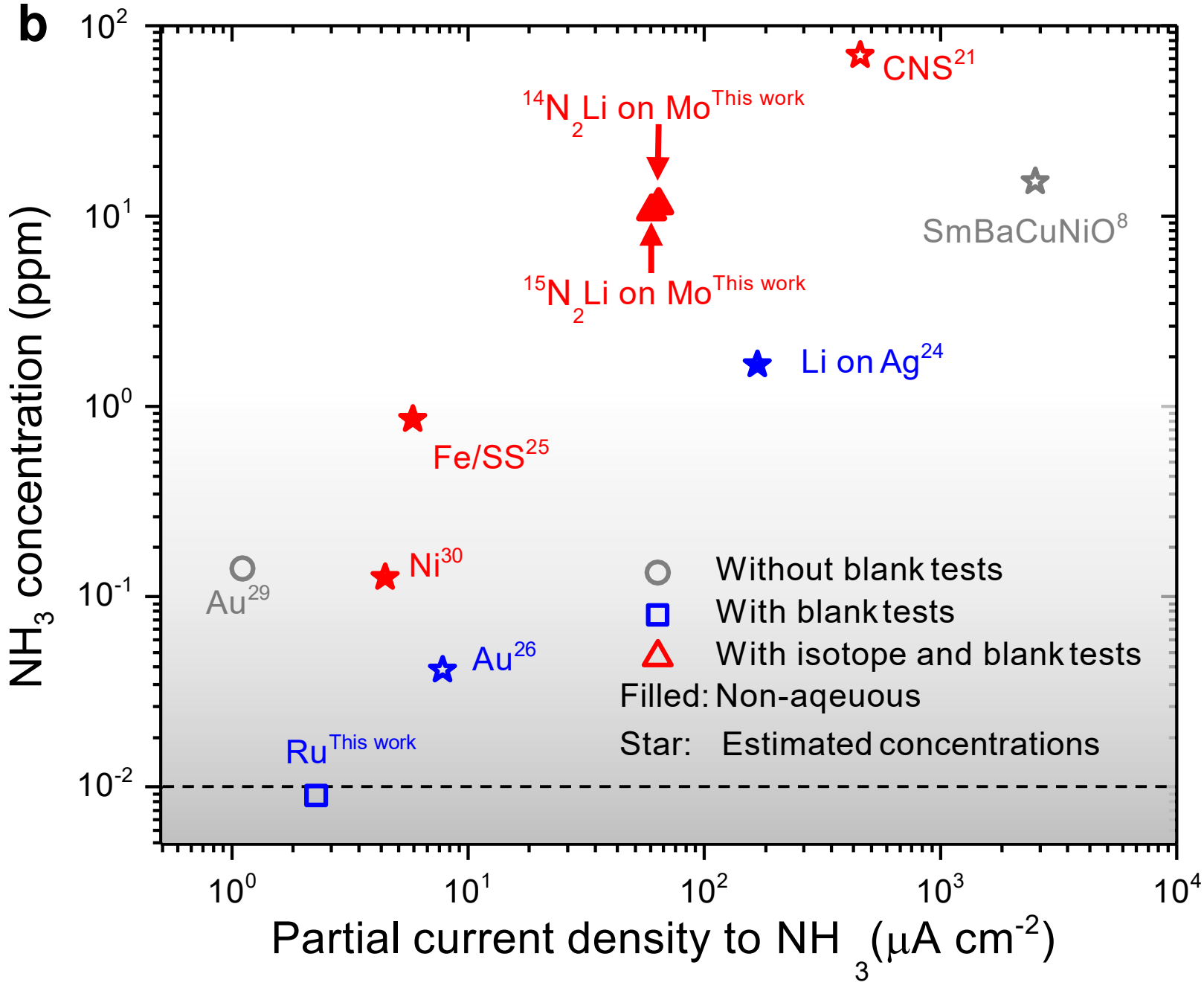
b
10^2
10^1
10^0
10^{-1}
10^{-2}
NH_3 concentration (ppm)
$^{14}N_2$Li on Mo This work
$^{15}N_2$Li on Mo This work
CNS[21]
SmBaCuNiO[8]
Li on Ag[24]
Fe/SS[25]
Ni[30]
Au[29]
Au[26]
Ru This work
Without blank tests
With blank tests
With isotope and blank tests
Filled: Non-aqeuous
Star: Estimated concentrations
10^0
10^1
10^2
10^3
10^4
Partial current density to NH_3 ($\mu A\ cm^{-2}$)

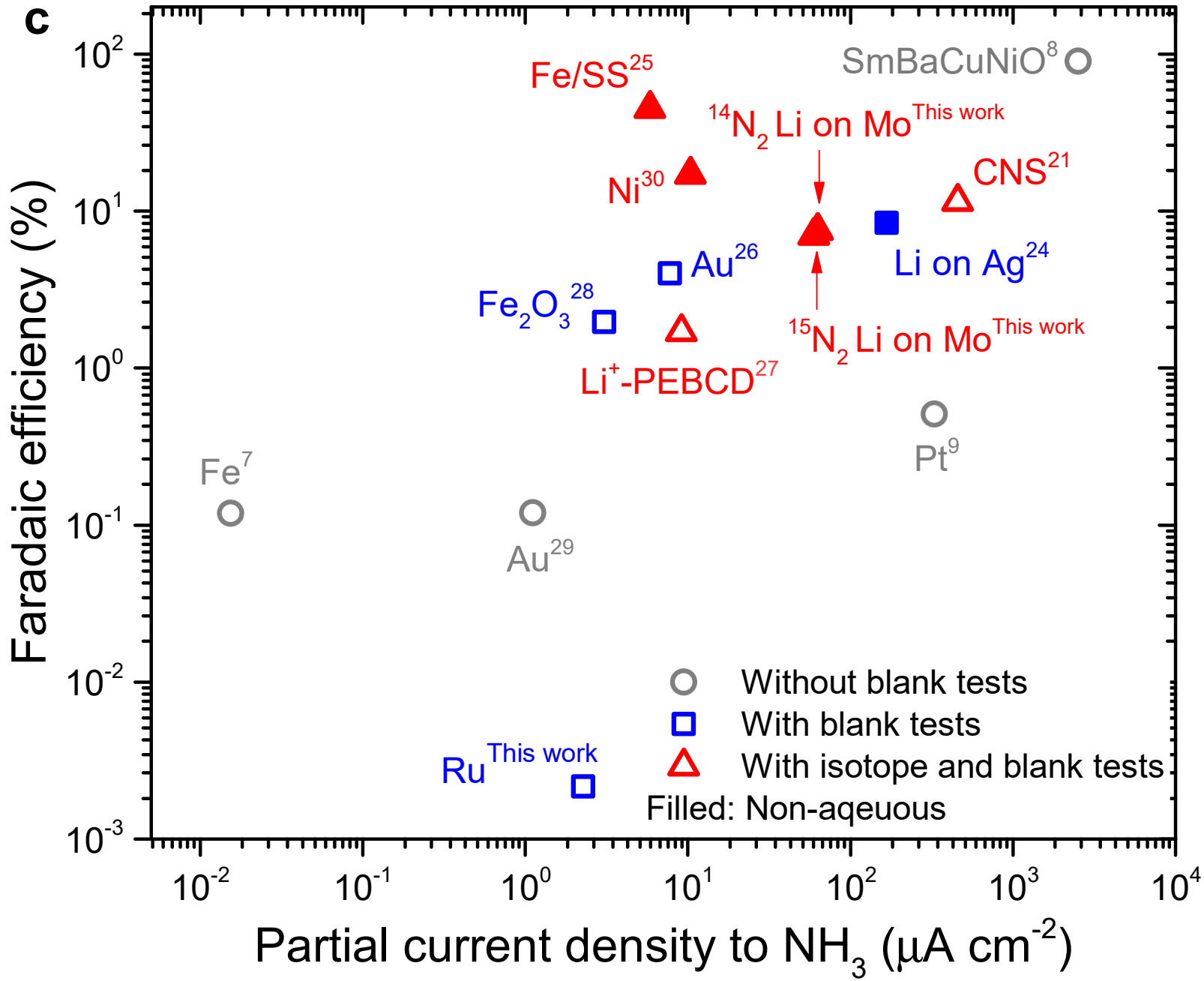
c
Faradaic efficiency (%)
Partial current density to NH3 (μA cm-2)
Fe/SS25
SmBaCuNiO8
14N2 Li on Mo This work
Ni30
CNS21
Au26
Li on Ag24
Fe2O3 28
15N2 Li on Mo This work
Li+-PEBCD27
Pt9
Fe7
Au29
Ru This work
Without blank tests
With blank tests
With isotope and blank tests
Filled: Non-aqeuous

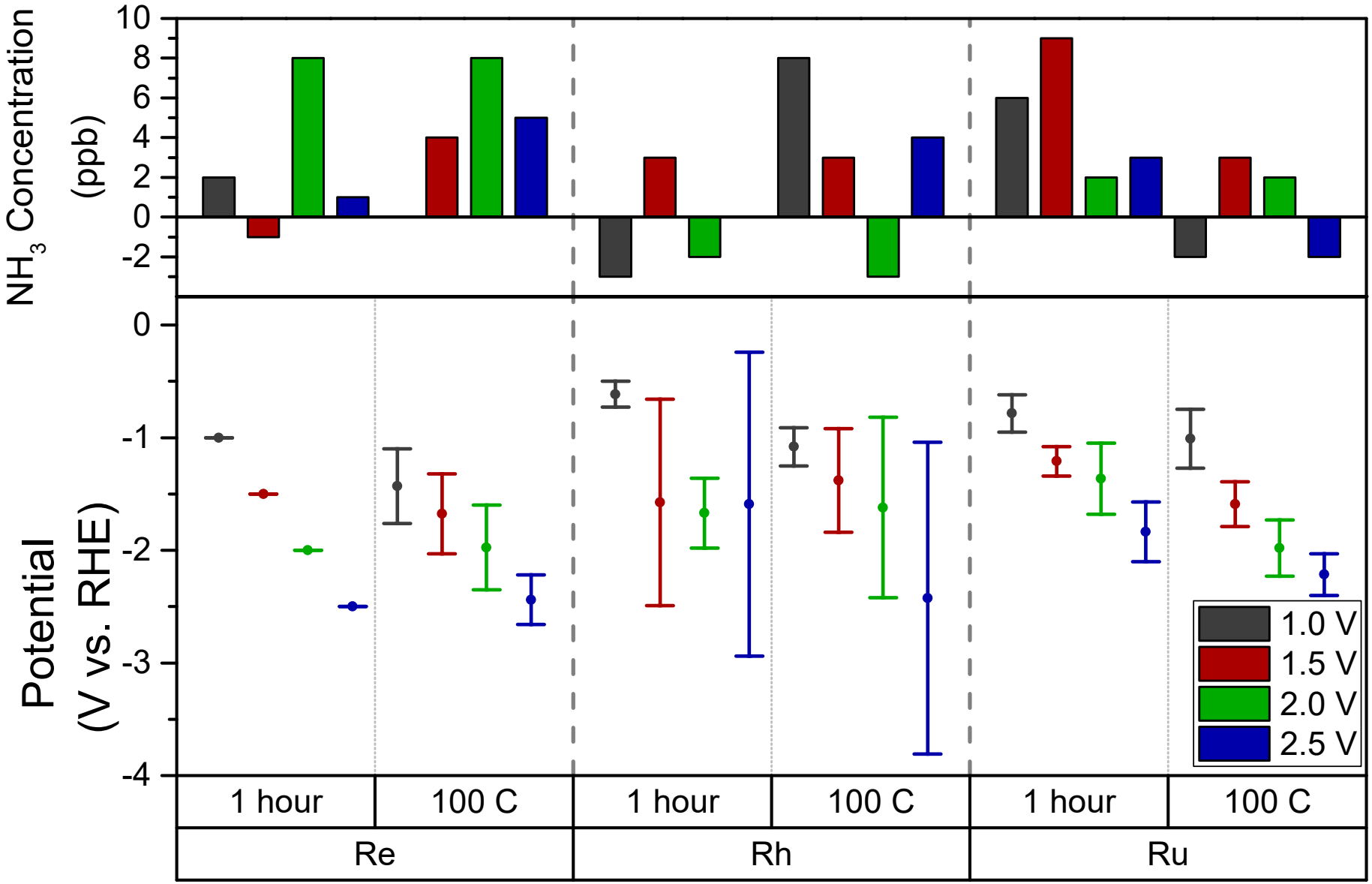
NH3 Concentration
(ppb)
10
8
6
4
2
0
-2
Potential
(V vs. RHE)
0
-1
-2
-3
-4
1.0 V
1.5 V
2.0 V
2.5 V
1 hour
100 C
1 hour
100 C
1 hour
100 C
Re
Rh
Ru

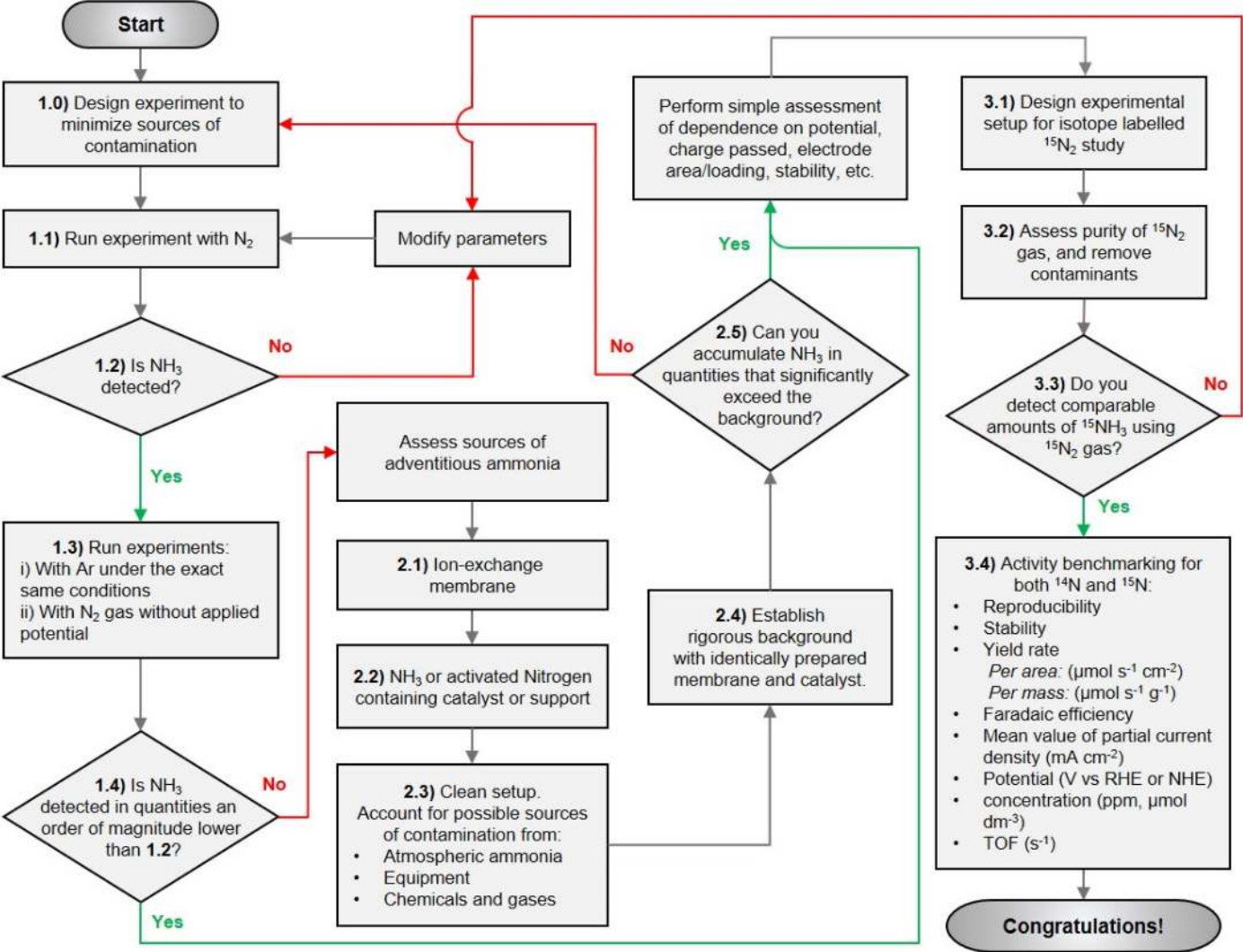
Start
1.0) Design experiment to minimize sources of contamination
1.1) Run experiment with N_2
Modify parameters
1.2) Is NH_3 detected?
No
Yes
1.3) Run experiments:
i) With Ar under the exact same conditions
ii) With N_2 gas without applied potential
1.4) Is NH_3 detected in quantities an order of magnitude lower than 1.2?
No
Yes
Assess sources of adventitious ammonia
2.1) Ion-exchange membrane
2.2) NH_3 or activated Nitrogen containing catalyst or support
2.3) Clean setup. Account for possible sources of contamination from:
• Atmospheric ammonia
• Equipment
• Chemicals and gases
2.4) Establish rigorous background with identically prepared membrane and catalyst.
2.5) Can you accumulate NH_3 in quantities that significantly exceed the background?
No
Yes
Perform simple assessment of dependence on potential, charge passed, electrode area/loading, stability, etc.
3.1) Design experimental setup for isotope labelled $^{15}N_2$ study
3.2) Assess purity of $^{15}N_2$ gas, and remove contaminants
3.3) Do you detect comparable amounts of $^{15}NH_3$ using $^{15}N_2$ gas?
No
Yes
3.4) Activity benchmarking for both ^{14}N and ^{15}N:
• Reproducibility
• Stability
• Yield rate
Per area: (μmol s^{-1} cm^{-2})
Per mass: (μmol s^{-1} g^{-1})
• Faradaic efficiency
• Mean value of partial current density (mA cm^{-2})
• Potential (V vs RHE or NHE)
• concentration (ppm, μmol dm^{-3})
• TOF (s^{-1})
Congratulations!

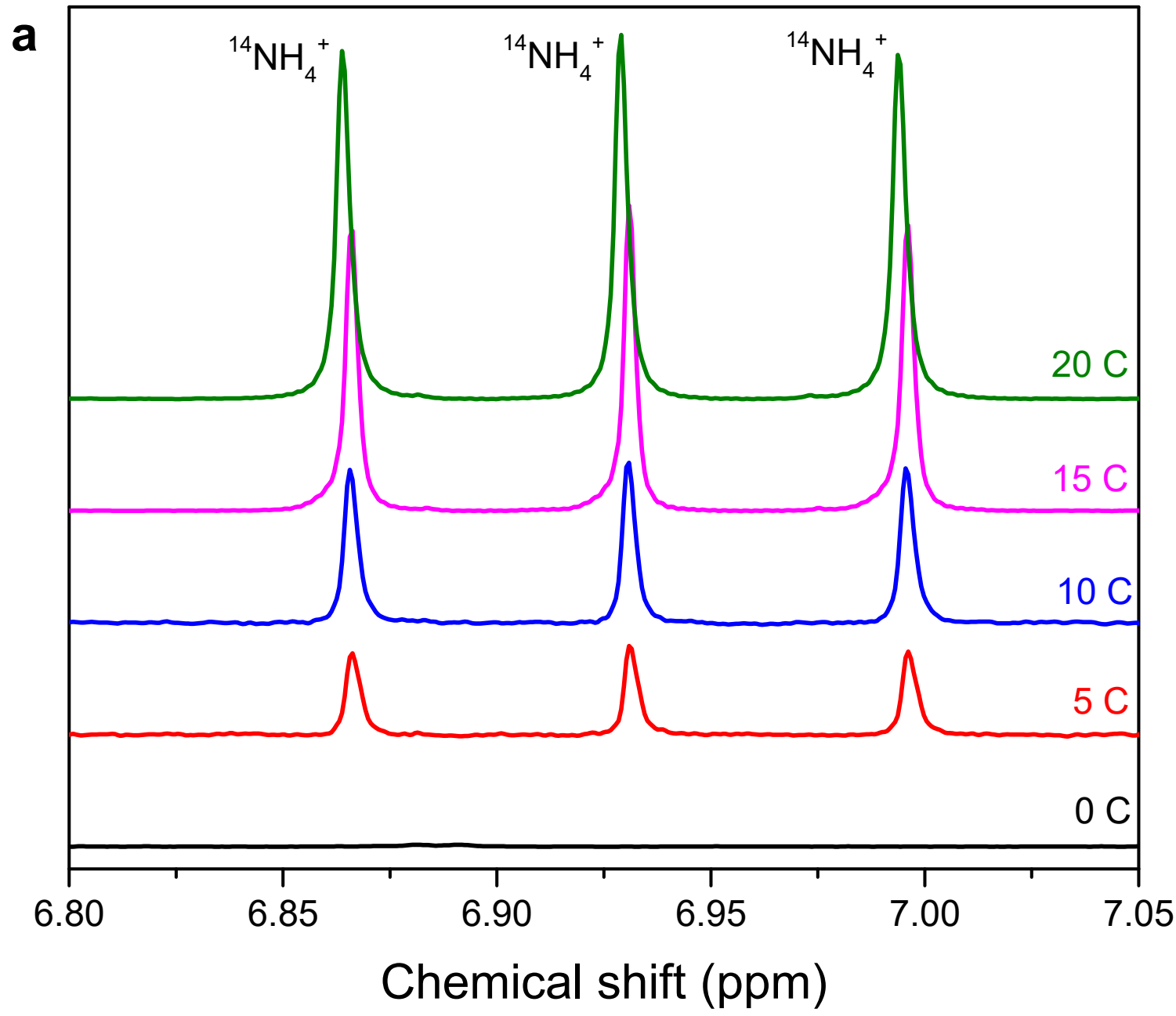
a
$^{14}NH_4^+$
$^{14}NH_4^+$
$^{14}NH_4^+$
20 C
15 C
10 C
5 C
0 C
6.80
6.85
6.90
6.95
7.00
7.05
Chemical shift (ppm)

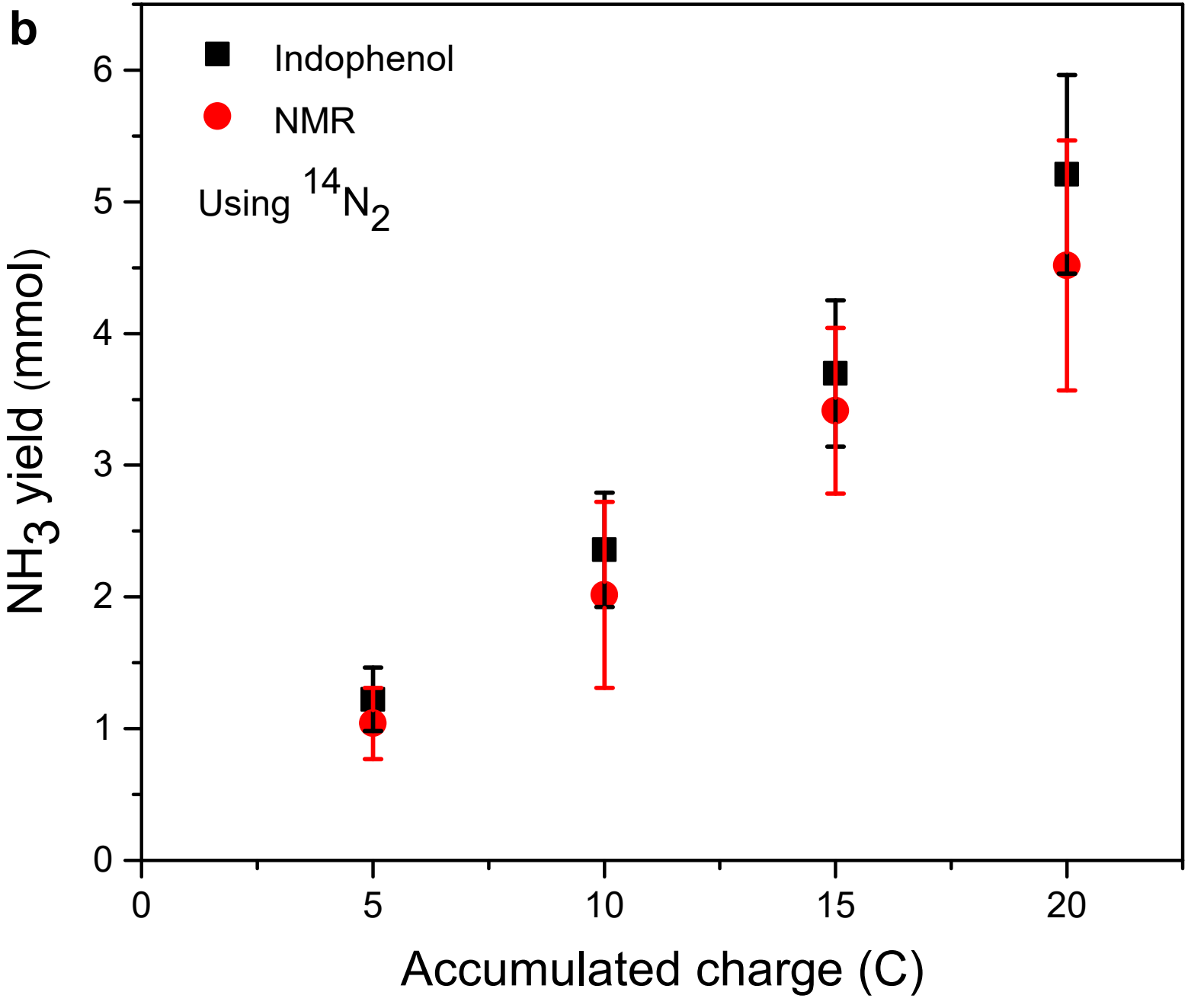
b
Indophenol
NMR
Using $^{14}N_2$
NH_3 yield (mmol)
0
1
2
3
4
5
6
0
5
10
15
20
Accumulated charge (C)

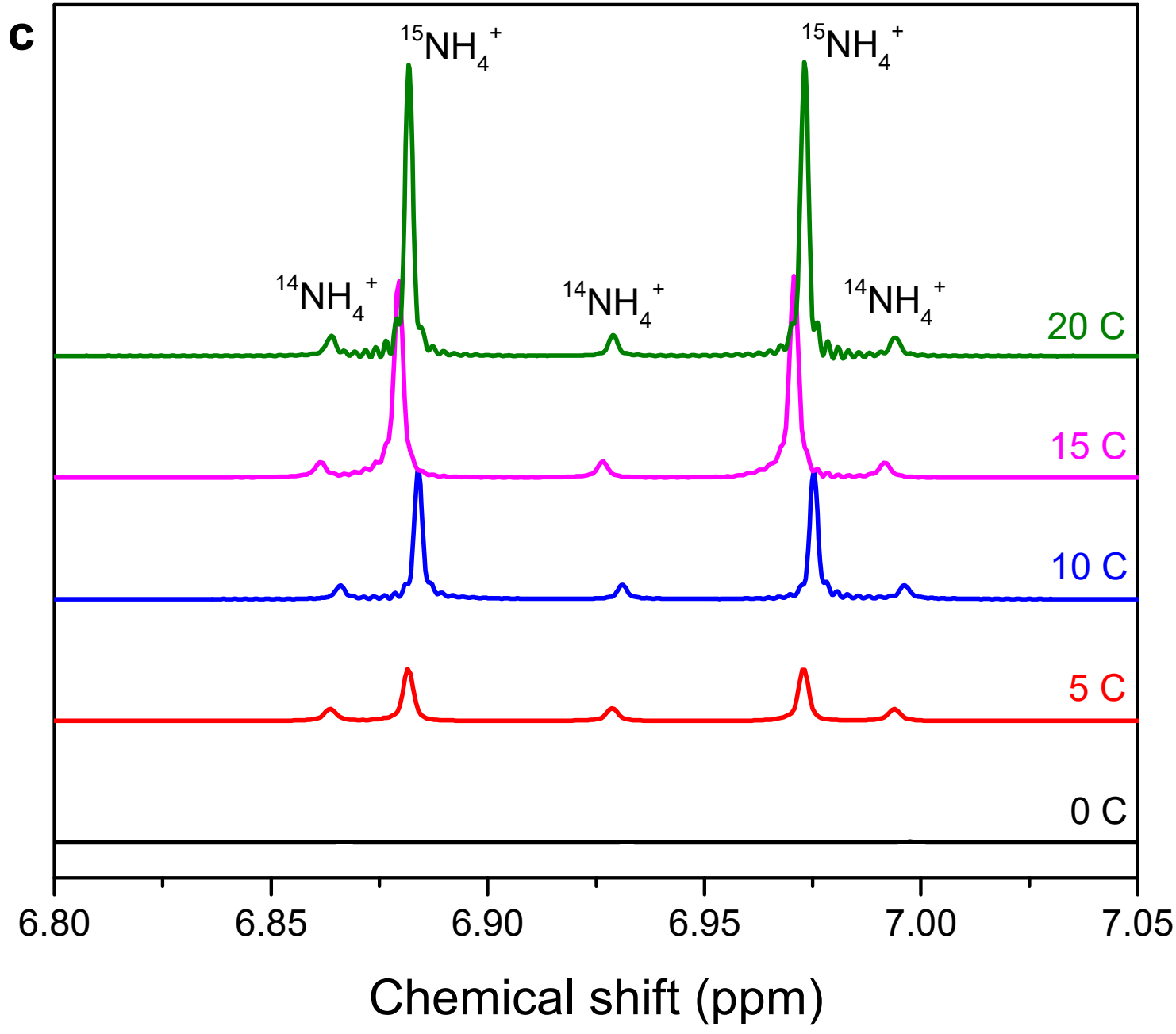
c
$^{15}NH_4^+$
$^{15}NH_4^+$
$^{14}NH_4^+$
$^{14}NH_4^+$
$^{14}NH_4^+$
20 C
15 C
10 C
5 C
0 C
6.80
6.85
6.90
6.95
7.00
7.05
Chemical shift (ppm)

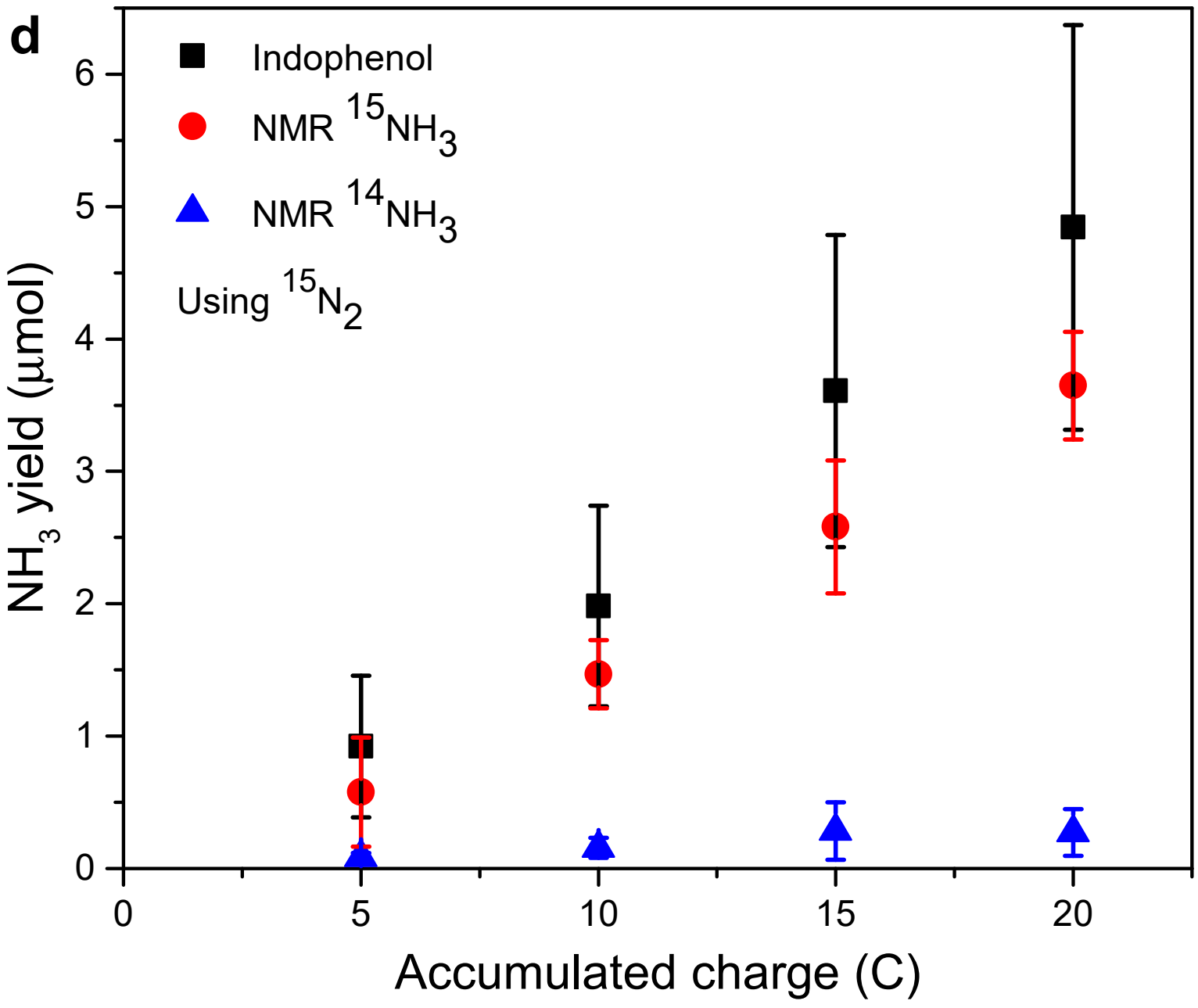
d
Indophenol
NMR $^{15}NH_3$
NMR $^{14}NH_3$
Using $^{15}N_2$
NH_3 yield (μmol)
0
1
2
3
4
5
6
0
5
10
15
20
Accumulated charge (C)